Applied Clay Science 214 (2021) 106274

Contents lists available at ScienceDirect

Applied Clay Science

journal homepage: www.elsevier.com/locate/clay

Coupling of chemical and hydromechanical properties in bentonite: A new reactive transport model

Andreas Jenni [a,*], Johannes C.L. Meeussen [b], Tapani A. Pakkanen [c], Janne T. Hirvi [d], Bukunmi Akinwunmi [d], Ángel Yustres [e], Vicente Navarro [e], Rubén López-Vizcaíno [e], Eveliina Muuri [f], Mika Niskanen [f], Paul Wersin [a], Urs Mäder [a]

[a] Institute of Geological Sciences, University of Bern, Baltzerstrasse 1+3, 3012 Bern, Switzerland
[b] NRG, Westerduinweg 3, 1755 LE Petten, the Netherlands
[c] Laboratory of Inorganic Chemistry, Environmental and Chemical Engineering, University of Oulu, P.O. Box 3000, 90014 Oulu, Finland
[d] Department of Chemistry, University of Eastern Finland, P.O. Box 111, Joensuu 80101, Finland
[e] Geoenvironmental Group, Civil Engineering Department, University of Castilla-La Mancha, Avda. Camilo José Cela s/n, 13071 Ciudad Real, Spain
[f] Posiva Oy, Olkiluoto, 27160 Eurajoki, Finland

ARTICLE INFO

Keywords:
Chemomechanical modelling
Compacted bentonite
Reactive transport
Radioactive waste repository
Swelling pressure
Engineered barrier

ABSTRACT

The reactive transport framework ORCHESTRA was used to implement a dual porosity reactive transport system that accounts for mechanical processes relevant for confined swelling clays at full saturation. The new implementations are based on water retention data generated by molecular dynamics simulations, and on fundamental mechanical formulations. The code predicts and fully couples porewater chemistry, exchanger population, diffusive transport, mineral reactions, volume fractions of the free and Donnan porosity domains, and swelling pressure. The chemomechanical predictions were compared with experimental measurements of swelling pressure and d-value of the clay in different chemical environments. A simulation of bentonite in contact with a constant concentration reservoir demonstrates the performance of the new model approach. It can be used to model interactions of bentonite with different groundwaters or cement and steel.

1. Introduction

Effective diffusion coefficients in bentonite, and properties like swelling pressure or hydraulic conductivity are crucial for most engineered barrier systems of radioactive waste repositories. Swelling pressure severely affects the stress field in the deposition hole after closure. The transport properties control not only the migration of radionuclides possibly released from the canister, but also the interaction of the canister with cement or groundwater outside the bentonite. These properties depend on the porewater composition and the clay's exchanger population (Glaus et al., 2010; Jenni and Mäder, 2018; Karnland et al., 2006; Van Loon et al., 2007). The osmotic suction and, consequently, the chemical environment of the bentonite, significantly influence its performance at full saturation. The equilibration of the bentonite's porewater with a new external porewater chemistry changes its swelling pressure, pore size distribution, and therefore, its transport properties (Karnland et al., 2006; Kozaki et al., 1998; Kozaki et al., 2008; Kozaki et al., 2010).

The strong coupling and feed-back between chemical and physical parameters is caused by the swelling properties of montmorillonite, the major compound of bentonite. The d-value of this phyllosilicate varies with density, but also with the porewater composition outside and inside the interlayer. Apart from the changing water content in the interlayer, it contains exchangeable cations, which compensate the constant negative charge of the clay sheets. The nature of these cations obviously also influences the d-value. If the total volume of the bentonite is confined, the repulsion of the clay sheets leads to a swelling pressure, which strongly depends on the d-value. Therefore, chemical and physical local equilibrium conditions need to be solved at the same time. In case the chemical environment changes at constant total volume condition of the clay, reactive transport codes that consider the interaction of chemical and hydromechanical properties (CM coupling) are capable of modelling mineral reactions, equilibration times, and changes in swelling pressure (Yustres et al., 2017). Such predictions are beneficial

* Corresponding author.
E-mail address: andreas.jenni@geo.unibe.ch (A. Jenni).

https://doi.org/10.1016/j.clay.2021.106274
Received 18 April 2021; Received in revised form 31 August 2021; Accepted 4 September 2021
Available online 14 September 2021

for the performance evaluation of bentonite used in an engineered barrier system envisaged for radioactive waste repositories (Wersin and Kumpulainen, 2017).

Many reactive transport codes simplify the influence of the clay surface charge on the porewater composition. For example, anion exclusion can be approximated in single porosity transport approaches by averaging the effective diffusion coefficients of anions and cations (Berner et al., 2013; Fernández et al., 2009; Kosakowski and Berner, 2013; Wallis et al., 2016), or by assigning species-dependent effective diffusion coefficients in addition to the different coefficients in pure water (e.g., Samper et al., 2018; Zheng et al., 2020). However, as soon as mineral reactions change the porosity, or the swelling behaviour changes, these simplifications fail in predicting subsequent changes in transport. A dual porosity approach can handle such scenarios: in this case, the total porosity was segmented into a homogeneous porosity fraction where the ions in the porewater are affected by the clay surface charge (*Donnan porosity*), and into a charge-balanced *free porosity* distant from the clay sheet surfaces (Jenni et al., 2017).

In the new model approach presented here, ionic strength (via osmotic suction) and the cations in the interlayer influence the clay's d-value and therefore the volume of the Donnan porosity. Although direct measurements of these mechanisms are scarce, many indirect indications exist (Jenni et al., 2019). Diffusion in the Donnan porosity is different from diffusion in the free porosity, and the Donnan porosity contains almost no anions. Therefore, changes in the two porosity domains affect total transport, and also affect swelling pressure. Classic hydromechanical and reactive transport models neglect these effects, which only slightly influence transport and swelling pressure compared with the influences of density and degree of saturation. However, the effect of large changes in ionic strength (Jenni and Mäder, 2018), or porosity clogging (Chagneau et al., 2015), can be significant and is not predicted by classic approaches.

The coupling between porewater chemistry, mechanical clay properties, and transport was implemented in the multicomponent reactive transport code ORCHESTRA (dual porosity version), as described in the following. The implementation was greatly facilitated by the fact that ORCHESTRA allows user-defined expressions and equations to be added to the chemical solver input file, and this was used in combination with standard object classes for Donnan model and equilibrium chemistry.

A fully coupled reactive transport example demonstrates the effects of porewater chemistry and mineral reactions on the volume fractions of the two porosity domains, influencing diffusive transport and swelling pressure.

2. Model description

2.1. Dual porosity reactive transport

Meeussen (2003) provided the general features of ORCHESTRA (open source available from Meeussen, 2021) and Steefel et al. (2014) compared ORCHESTRA capabilities with other codes. The code was extended with multi-component transport and benchmarked extensively (Marty et al., 2015). For this work the most important feature of ORCHESTRA is that it allows users to add their own variables, expressions and equations to a "chemical" system, and to combine these with the standard set of chemical models that is available in the standard model library. In this way the tight coupling of chemical and physical processes discussed here can be solved in a single iteration loop. Furthermore, the standard phase objects make it relatively easy to subdivide a chemical system in different compartments (e.g. Donnan and free porewater), where ions have different (transport) properties.

Minerals reacted kinetically to attain thermodynamic equilibrium with the free porewater. Subsequent porosity changes influenced diffusive transport based on Fick's law, which was extended with the Nernst-Planck formulation to maintain charge balance. Aqueous speciation, pH calculation, and activity corrections are implemented.

Although the single-porosity ORCHESTRA model version (charge-balanced free porewater only, no influence of surface-charge on porewater) can handle unsaturated systems, the current dual porosity version of the code was restricted to fully saturated conditions. The total porosity was divided into two homogeneous volumes. The porewater in the Donnan porosity contained an excess of cations balancing the negative charge of the clay sheets (Jenni et al., 2017, Fig. 1 in supplementary material). This porosity contained the water in the clay interlayers plus the water on clay outer particle surfaces (often called diffuse double layer).

The chemical composition of this porewater was calculated by assuming Donnan equilibrium between the anion-depleted porosity and the remaining fraction of the total porosity which is referred to as freely accessible porosity, free porosity in short. Donnan equilibrium assumed a uniform composition of the pore water in the anion-depleted porosity (Donnan porosity). For the purpose of simplification, activity coefficients in the Donnan porosity were set equal to the free porosity (Tournassat and Appelo, 2011), and the equilibrium was written with concentrations for species i as

$$c^i_{Donnan} = c^i_{free}\ exp\left(\frac{-z^i\ F\ \psi_{Donnan}}{R\ T}\right) \quad (1)$$

where c is the concentration in the two porosity domains [mol/L], z is the charge number [−], F is the Faraday constant, ψ_{Donnan} is the Donnan potential [V], R is the gas constant [J/mol/K], and T is the temperature [K] (Tournassat and Appelo, 2011). Total charge of all Donnan species balanced the surface charge [eq/L Donnan porewater], which is related to the cation exchange capacity (CEC) [eq/kg dry clay]. Eq. (1) represents the average pore water composition close to a charged surface derived from the integration of the more rigorous Poisson-Boltzmann formulation (Tournassat and Steefel, 2015). Because these formulations predict a minor content of anions in this porosity, the often used term anion-free or anion-restricted porosity is not appropriate within this concept. In the present work, this porosity is called *Donnan porosity*, in contrast to the *free porosity* in which the porewater is internally charge-balanced (called free porewater).

Diffusive transport was considered in both porosity domains with different geometric factors, and the two resulting fluxes add up to the total diffusive flux (Jenni et al., 2017). The effective diffusion coefficient for each porosity domain and species i was written as (Flury and Gimmi, 2002)

$$D^i_{eff,free} = G_{free}\ n_{free}\ D^i_0 \quad (2)$$

$$D^i_{eff,Donnan} = G_{Donnan}\ n_{Donnan}\ D^i_0 \quad (3)$$

where D_0 is the diffusion coefficient in water (different for each species i, but equal in free and Donnan porewater), and G is the geometric factor of the free and Donnan porosity n, respectively. G_{free} was considered to be equal for all species in the free porosity, as well as G_{Donnan} in the Donnan porosity (note that the distinction of two separate geometric factors, which may be difficult from a conceptual point of view, is a consequence of assuming two parallel fluxes in the dual porosity approach). A similar dual porosity approach is also implemented in PhreeqC and CrunchFlowMC (Alt-Epping et al., 2015), now called CrunchClay. In all these codes, G_{free} and G_{Donnan} are crucial parameters constraining diffusive transport, depending on the microstructure of the material and total porosity (and connected dry density). In all approaches, they are kept constant during the simulation, which might be justified if only small changes in total porosity occur during the simulation.

Reactive minerals were implemented in ORCHESTRA either kinetically following any rate law with possible dependencies on any aqueous species, or as non-kinetic mineral in explicit equilibrium at any time with the free porewater. The latter is applicable in case of fast reacting,

transport-controlled systems like cement. It saves computing power, and allows for large time steps. In addition, inert minerals can be defined. No mineral precipitation occurred in the Donnan porosity. The limited space in the clay interlayer might inhibit nucleation and precipitation of minerals. This is supported by the experiment of Chagneau et al. (2015), where clogging stopped anion diffusion (free porosity presumably fully clogged), but only slowed down neutral species by half (still mobile in the Donnan porosity).

The present code version coupled transport and porosity. Following Eqs. (2) and (3), the effective diffusion coefficients depended linearly on free and Donnan porosity, Archie's law was not implemented. Any volume change caused by mineral dissolution/precipitation was compensated by the total porosity. Clogging could occur up to a chosen threshold value. In contrast, the Donnan porosity could not be clogged, because the code did not allow for mineral precipitation in this domain (see above).

The Donnan and free pore volume were both present in the same "mixed cell" in the current ORCHESTRA model set-up. This made it possible to dynamically calculate the ratio between these volumes based on the chemical composition of the pore water. Because the total effective mobility of components/ master species between two neighbouring cells was calculated from the weighted average of species concentrations and charges in both Donnan and free porewater, no explicit definition of connectivities between these domains within a (finite volume) cell or with adjacent cells volumes was required (connectivity in dual porosity approaches is discussed in Tournassat and Steefel, 2015).

The dual porosity extension of ORCHESTRA was benchmarked by modelling the diffusion across a dual/single-porosity interface simulated with the FLOTRAN reactive transport code (Jenni et al., 2017). Mechanical and chemomechanical processes changed both Donnan and free porosity volumes (section below), and also influenced diffusive transport similarly to mineral reactions.

2.2. Chemomechanical coupling

2.2.1. Molecular dynamics data substituting water retention curves

Water retention curves and reference measurements of swelling pressure versus porosity provided the basis for several hydromechanical model approaches (Navarro et al., 2017b). These experimental data exist for clay materials in equilibrium with deionised water, mostly in the Na-exchanged form (referenced in the same publication). Salinity effects were then taken into account by quantifying osmotic suction in the free porewater. If ions were present in the free porewater, Eq. (1) predicted additional anions and cations in the Donnan porewater in excess of the cations that compensate the exchange capacity. The osmotic suction resulting from these additional ions was added to the suction in the Donnan porewater associated with deionised water (Navarro et al., 2017b). Approaches to handle Ca-exchanged and mixed Na-Ca clays were given in De la Morena et al. (2018).

Recent molecular dynamics (MD) calculations delivered data of repulsive forces between clay sheets at various Na-Ca-Cl concentrations in the external water (Akinwunmi et al., 2020a; Akinwunmi et al., 2020b). At elevated external ionic strength, additional ions could be observed between the clay sheets, in agreement with Eq. (1). Therefore, the resulting repulsive force included the osmotic effect of free porewater salinity (external water in the MD calculations), as well as the osmotic effect of all ions between the clay sheets.

Navarro et al. (2021) showed satisfying agreement between MD data of montmorillonite and experimentally derived retention curves for Na-bentonite (containing this montmorillonite) in equilibrium with NaCl solutions. For such comparisons, the MD data (clay sheet distances, repulsive forces, residence times of ions between and outside the clay sheets) was converted into a form comparable with retention curve data (porosities, swelling pressures), considering salinity effects as described above. These conversions were also needed if MD data replaced retention curves in chemomechanical models.

The large number of MD calculations published in Akinwunmi et al. (2020a) and Akinwunmi et al. (2020b) was converted and fitted by a complex function ($R^2 = 0.92$) in the general form (several different fitting functions were tested and double exponential was chosen, more information in the supplementary material)

$$\boldsymbol{P_{swell}} = \mathbf{f}\left(\boldsymbol{c_{Na,free}}, \boldsymbol{c_{Ca,free}}, \boldsymbol{d}\right) \tag{4}$$

This equation defines the swelling pressure P_{swell} exerted from parallel clay sheets with spacing d placed in an external solution with Na and Ca concentrations $c_{Na,\ free}$, $c_{Ca,\ free}$ (Cl anion base). In the new ORCHESTRA model version, this MD fitting function replaced the experimentally derived retention curve from Na-montmorillonite at zero ionic strength and the two osmotic suction components arising from salinity in the free porosity described above. Eq. (4) provides data on mixed Na-Ca systems.

2.2.2. Derivation of swelling pressure and porosity volumes

Additional relationships were needed to define d-value and swelling pressure. Navarro et al. (2021) suggested that at isochoric conditions any change in Donnan void ratio e_{Donnan} must be compensated by e_{free} and vice versa in case of constant total void ratio e_{total}.[1] In case of non-constant e_{total}, we write

$$\boldsymbol{e_{total}} = e_{free,ref} + \Delta e_{free} + e_{Donnan,ref} + \Delta e_{Donnan} \tag{5}$$

where $e_{Donnan,\ ref}$ and $e_{free,\ ref}$ are void ratio measurements at known swelling pressure $P_{swell,\ ref}$. These reference values were derived from the same material for which the chemomechanical behaviour was predicted (e.g., bentonite), but at any dry density at zero ionic strength in its Na form. Navarro et al. (2017a) further suggested

$$\Delta e_{free} = -k \bullet \ln \frac{P_{swell}}{P_{swell,ref}} \tag{6}$$

with k being the macrostructural elastic stiffness (Alonso et al., 1990). d-value and e_{Donnan} were related by the montmorillonite surface area (internal and external) and the montmorillonite grain density (Holmboe et al., 2012; Tournassat and Appelo, 2011). Combining Eqs. (4), (5), and (6) defined swelling pressure, d-value, and Donnan porosity. Total porosity was derived from the montmorillonite dry density and could vary due to dissolution or precipitation. At each time step, the updated total porosity resulting from mineral reactions was divided into Donnan and free porosity according to Eqs. (4), (5), and (6). Eq. (4) has no algebraic solution and was solved numerically at each time step, in the iteration process together with Eqs. (5) and (6) and all chemical equilibrium reaction equations.

2.2.3. Homogenisation

The calculations described above were applied to a homogeneous domain, e.g. a small cell in a finite volume approach. Swelling pressure gradients could arise from chemical or porosity gradients in a larger domain partitioned into cells and could be handled by the model only in two ways in a 1D domain: a) instant equalisation of swelling pressure by adapting total porosities and transferring solid mass between the cells (homogenisation), or b) the swelling pressure gradient remained. Experimental observations indicated that homogenisation of dry density gradients (and connected swelling pressure gradients) at equal porewater chemistry was time-dependent and stopped at low pressure gradients (Dueck et al., 2018). In the current ORCHESTRA version, swelling pressure gradients were not equalised (no instantaneous homogenisation). However, diffusive transport tends to homogenise porewater

[1] Most reactive transport codes use porosity n (pore volume fraction of total volume), whereas void ratio e (pore volume/ total solid volume) is more common in mechanical models. Conversion is trivial: $e = n/(1\text{-}n)$.

chemistry over time, which finally also equilibrates swelling pressure in most systems (e.g., Section 4).

2.2.4. Multimineral materials

In case of multimineral systems with montmorillonite as major component, its swelling pressure was assumed to be equal to the pure montmorillonite with a dry density identical to the effective montmorillonite dry density of bentonite (EMDD, the dry density of the montmorillonite in between the accessory minerals, Dixon et al., 2002). This was shown experimentally up to 30–40% of accessory minerals, which must be homogeneously distributed in the clay matrix without forming a grain-supported microstructure (Ola Karnland, Clay Technology, unpublished). The reference measurement of $P_{swell,\ ref}$ at known porosities was taken from the corresponding purified clay material (matrix).

3. Comparison of experimental and modelled chemomechanical data

Only limited experimental data of swelling pressure at different dry densities and at equilibrium with different electrolytes are available. Many measurements in literature suffer from non-equilibrium or ill-defined conditions:

- From the onset of bentonite resaturation, gypsum (approx. 0.5–2 wt % in Wyoming-type bentonite) dissolved. The exchanger equilibrated with the additional Ca, and the free porewater was saturated with respect to gypsum. Long equilibration times were needed to dissolve all gypsum and to equilibrate the free porewater with the target electrolyte, and much longer time was needed to remove the additional Ca from the exchanger that originates from gypsum dissolution (Section 4). Otherwise, not the swelling pressure of a bentonite in equilibrium with the target electrolyte was measured, but of a bentonite with increased Ca occupancy and additional sulphate in the porewater. Furthermore, at constant total volume, porosity increased by the volume of the dissolved gypsum and simultaneously, EMDD decreased with respect to the target dry density. Especially at high densities, where the density/pressure curve is steep (Fig. 1), the swelling pressure was then significantly decreased (Jenni et al., 2019). Therefore, indicated boundary conditions of measured bentonite swelling pressures did not meet the experimental conditions: ionic strength of equilibrating electrolyte was actually higher, exchanger population was higher in Ca, and density was lower, e.g., non-purified Wyoming-type bentonite samples in Karnland et al. (2006) and Holmboe et al. (2012).
- Bentonite slurries compacted to the desired dry density exhibited a microstructure different from a dry-pressed core which was slowly resaturated through a filter (Seiphoori et al., 2014). Especially coarse-grained or pelletised bentonites showed very high initial free porosity if prepared in the former way, which is expected to decrease during slow homogenisation. Swelling pressures of such bentonites measured shortly after compaction differed significantly from swelling pressures of fine-grained bentonites saturated and equilibrated for weeks (Karnland et al., 2008; Hoffmann et al., 2007).
- Small inaccuracies of pressure cell volume and bentonite mass (bentonite squeezed through gaps between filters or pistons during swelling) potentially led to significant changes of the target dry density. Effective density should then be measured post mortem of the swelling pressure experiment, and small samples lead to high errors in this measurement. Minor changes of density cause significantly different swelling pressures especially at high densities, as argued above.

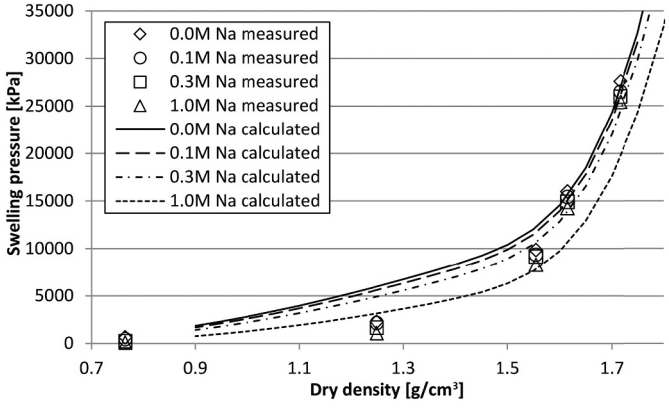

Fig. 1. Comparison of predicted swelling pressures of compacted Na-montmorillonite (lines) with measurements (Karnland et al., 2006) at different NaCl concentrations.

Karnland et al. (2006) circumvented these obstacles in the swelling pressure measurements of purified Wyoming-type bentonite (mostly montmorillonite), systematically available for different electrolytes at complete equilibration. The same constant volume sample cell was equilibrated at different ionic strengths, which ensures constant dry density. Continuous logging of the pressure until constant, and a close to constant reservoir chemistry ensured full equilibration. Different samples were used for Na- and Ca-montmorillonite. Therefore, these swelling pressures were compared here with the model predictions.

Measurements of d-value (which can be converted into Donnan porosity, see Section 2.2.2), of compacted, fully saturated clay samples are very scarce, even more scarce if equilibrated with different electrolytes. Although indirect measurements exist in form of different diffusion coefficients and hydraulic conductivities of clays in equilibrium with different electrolytes, the derivation of pore size distributions from these data requires a microstructural concept and complex transport models. To the best of our knowledge, only Kozaki et al. (1998b), Kozaki et al. (2008) and Kozaki et al. (2010) measured d-values in montmorillonite at different densities, in equilibrium with different NaCl concentrations, and at different Na-Ca exchanger occupancies. They found a clear d-value dependency on density and on NaCl concentration, but not on exchanger occupancies. The latter two dependencies, however, were only measured at 1 g/cm^3 dry density. All measurements resulted in smaller d-values at the indicated densities compared with other literature data (Holmboe et al., 2012), possibly due to incomplete saturation (Villar et al., 2012). Therefore, Holmboe et al. (2012) performed similar measurements with an improved analytical approach, but only with clays in equilibrium with deionised water. Accuracy and consistency of these data from montmorillonite made them most suitable for comparison with the model predictions.

Parameters needed in the model verification included the reference values $P_{swell,\ ref}$ at known dry density $D_{dry,ref}$, d_{ref}, and further material properties like montmorillonite grain density D_{grain} and montmorillonite surface area S (internal and external). In all cases, parameters were derived from Wyoming-type montmorillonite. Macrostructural elastic stiffness k is often used as fitting parameter. Navarro et al. (2015) and Navarro et al. (2017b) proposed $k = 0.1$, Navarro et al. (2017a) $k = 0.0729$ for Wyoming-type bentonite. Parameters used here are reported in Table 1.

Table 1
Parameters and their sources used in the chemomechanical part of the model for Wyoming-type bentonite.

Parameter	Value used in model	Source
$P_{swell,ref}$	9850 kPa	Karnland et al. (2006)
$D_{dry,ref}$	1.555 g/cm^3	Karnland et al. (2006)
d_{ref}	1.65 nm	Holmboe et al. (2012)
D_{grain}	2.8 g/cm^3	Tournassat and Steefel (2015)
S	756,000 m^2/kg	Holmboe et al. (2012)
k	0.07	Navarro et al. (2017a), adapted

The ORCHESTRA version extended with the CM coupling formulations and using the parameters above could predict swelling pressure and d-values in an equilibrium system. In parallel, the formulations could be solved with any numerical solver in full agreement with ORCHESTRA results (validated in Microsoft Excel 2010 using the built-in solver add-in with GRG nonlinear solving method).

Only the primary species Na^+, K^+, Ca^{+2}, Mg^{+2}, Al^{+3}, Fe^{+3}, H_4SiO_4, Cl^-, SO_4^{-2}, and Tracer were considered, without any secondary species. Depending on the equilibrium system, the required concentrations were assigned to Cl^-, Na^+ or Ca^{+2}, all other species were set to 1×10^{-9} M. No transport occurred in this equilibrium calculations.

Model predictions of swelling pressures at different dry densities agreed well with measured values (Fig. 1). No measurement errors were available, but a systematic error must be expected. Errors in the dry density measurement would shift one ionic strength series by the same amount, because one series originated from the same sample, but maintain the differences of the values within the series. The model overestimated the measured pressures at 1.25 g/cm^3 dry density. This may be related to the underlying MD simulations, which tended to overestimate swelling pressures especially at low dry densities compared to real experimental values (Sun et al., 2015). But such low measured pressures were prone to larger errors compared to higher pressures, depending on the experimental set-up. However, the model captured the smaller pressures at higher ionic strengths. The higher the ionic strength, the higher the osmotic suction, and the lower the chemical potential of the free water. Therefore, less water will pass into the Donnan porosity and less swelling will occur.

Fig. 2 compares d-values in Na-montmorillonite predicted by the model with measurements. Predictions agreed very well with the most recent XRD measurements performed on Na-montmorillonite by Holmboe et al. (2012). Fig. 3 compares the predictions with all measurements from Holmboe et al. (2012) and emphasises experimental uncertainties: different sample preparation methods influenced the results (subscripts C for saturation in a confined cell from the aqueous phase, Ads, Des for water adsorption or desorption of unconfined montmorillonite at different relative humidities). Differences between Na and Ca montmorillonite were within these differences caused by sample preparation.

In case of Ca-montmorillonite, the predicted swelling pressures generally fit the measurement trend (Fig. 4). Pressures were lower with increasing ionic strength. Only at 1.0 M and densities above 1.5 g/cm^3, predicted pressures were significantly lower than the measured data.

Predicted d-values agreed with measured values (Fig. 3). Both predicted and measured d-values of Ca-montmorillonite were close to the Na values at zero ionic strength.

4. Model application

A bentonite core containing reactive gypsum in contact with a constant concentration reservoir was modelled at isochoric conditions with the ORCHESTRA dual porosity reactive transport code including the chemomechanical implementation. Only gypsum could dissolve or precipitate with a reaction rate constant of $K = 10^{-2.79}$ mol/m^2/s (Palandri and Kharaka, 2004) and a reactive surface area of 0.1 m^2/g, following the transition state theory rate law without any additional dependencies (Lasaga, 1981; Lasaga, 1984). Inert accessory minerals were represented by "quartz" and "inertvolume". Only the primary species given in Section 3 were considered. The model approach presented in Section 2.2 and its verification for Na-Ca-Cl systems had to be extended to include the presence of sulphate. The MD fitting function (Eq. (4)) depends on Na and Ca concentrations in the free porewater and assumes Cl as only charge-balancing anion. Therefore, if additional anions were present, their effect on swelling properties was considered to be equal to the effect of the concentration of Cl, multiplied by their absolute charge. Thanks to this approximation, no extension of the formalism for Cl systems was needed for additional anions. Extending the Na-Ca-Cl system for more complex chemistries is further discussed in Section 5.

Fig. 5 shows the initial volume fractions with the constant concentration reservoir consisting of exclusively free porosity on the left, and a closed boundary condition on the right. The bentonite (35 cm in 1D) was represented by 25 cells of 14 mm in x direction and a volume of 0.14 L each. The classic montmorillonite stoichiometric formula was represented here by pyrophyllite (the TOT sheets only of montmorillonite), plus the Donnan porewater representing the interlayer water and the exchangeable cations. The use of pyrophyllite neglected the replacement

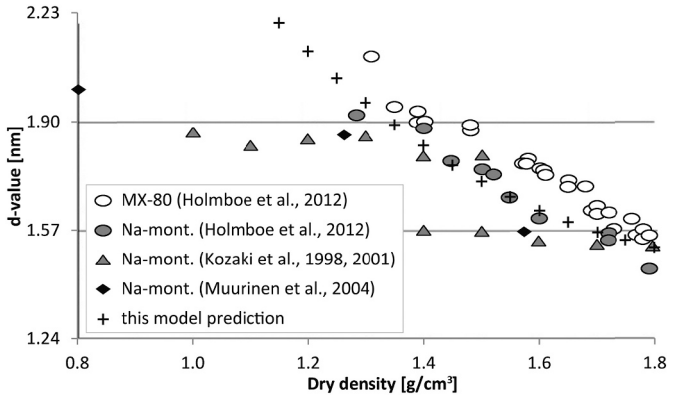

Fig. 2. Comparison of predicted d-values of compacted Na-montmorillonite (Na-mont.) with measurements (compiled by Holmboe et al., 2012).

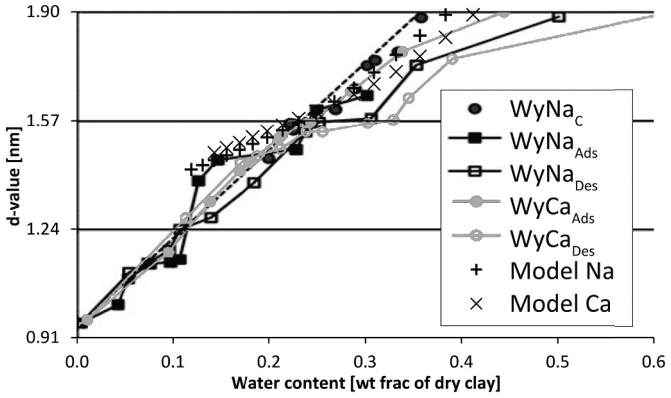

Fig. 3. Comparison of predicted d-values of compacted Na- and Ca-montmorillonite equilibrated at zero ionic strength with measurements of Holmboe et al. (2012).

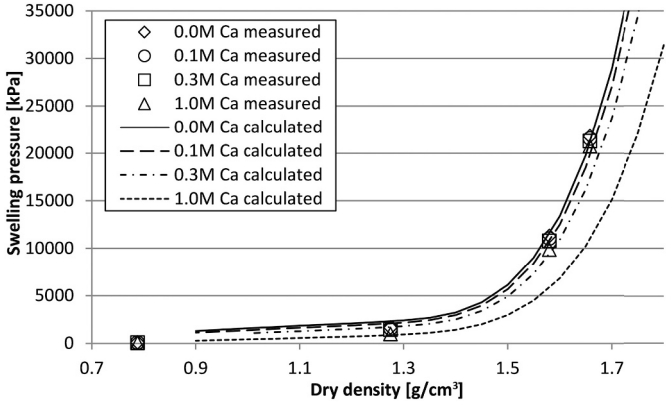

Fig. 4. Comparison of predicted swelling pressures of compacted Ca-montmorillonite (lines) with measurements (Karnland et al., 2006) at different $CaCl_2$ concentrations.

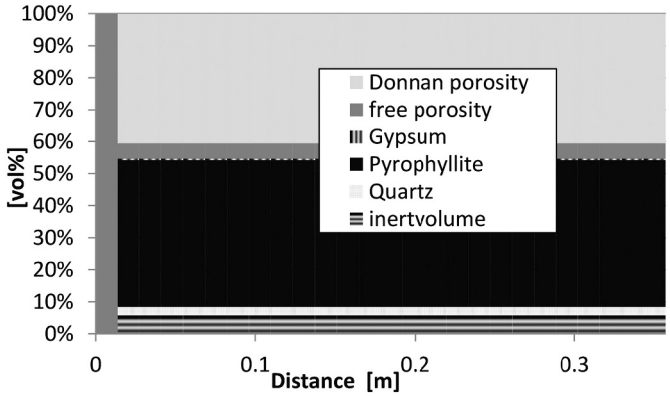

Fig. 5. Initial volume fractions with the constant concentration reservoir on the left (free porewater only), in contact with the bentonite core and the closed boundary on the right.

of some Al and Si by Mg or Fe in the TOT sheet and the resulting negative charge of the mineral. This assumption did not affect porewater concentrations as long as pyrophyllite was considered as inert as assumed here. Free porewater and reservoir had equal concentrations (0.04857 M NaCl), except for a difference in neutral tracer (Fig. 6). The Donnan porewater was in equilibrium with the free porewater and therefore consisted of Na balancing the CEC of 1.073 eq/kg dry montmorillonite (Yustres et al., 2017), and a marginal Cl concentration. The Donnan porewater concentrations replaced the ion population of the CEC in the classic clay concept. At the chosen porewater chemistry and the EMDD of 1.408 g/cm^3 (bentonite dry density 1.514 g/cm^3), the code predicted 8.23 MPa swelling pressure and 1.816 nm d-value, in general agreement with Karnland et al. (2006) and Holmboe et al. (2012) (Fig. 1, Fig. 2). Diffusive transport parameters were chosen in accordance with Jenni and Mäder (2018) and Yustres et al. (2017) (geometric factors of 0.1 and 0.01 in free and Donnan porosity, respectively, and diffusion coefficients in free water as stated therein).

Because the free porewater was undersaturated with respect to gypsum, it dissolved across the entire core until saturation in the free porewater was reached (Fig. 2 in supplementary material). The Donnan equilibrium between free and Donnan porewater chemistry predicted most Ca to be taken up by the Donnan porewater, and releasing Na into the free porewater. In contrast, sulphate was barely taken up by the Donnan and accumulated in the free porewater. The Ca removal from the free porewater led to a sulphate concentration above the concentration at gypsum saturation, in agreement with model predictions presented in Jenni and Mäder (2018). Ca and anion contents in the Donnan porewater were still too low to be visible in Fig. 2 (supplementary material). Due to the large differences in absolute ion contents of the free and the Donnan porewater (high CEC), small changes in the Donnan strongly affected free porewater composition.

The increase in ionic strength decreased swelling pressure and d-value. Gypsum dissolution and simultaneous porosity increase (EMDD decrease) also decreased swelling pressure, but increased d-value to a smaller extent. In parallel, Ca and sulphate from dissolved gypsum diffused into the constant concentration reservoir on the left. The resulting salinity gradient led to higher swelling pressure towards the reservoir.

Ongoing ion diffusion into the reservoir pushed the gypsum dissolution front to the right (Fig. 7). Swelling pressure and d-value adapted to both the ionic strength, change in Na/Ca, and increasing porosity (decreasing d-value). The superimposition of the chemical and physical effects on microstructure was reflected by the step in d-value up to 0.2 m from the reservoir: within 0–0.1 m, EMDD was constant (complete gypsum removal), and decreasing d-value was quasi-linear following the quasi-linear ionic strength decrease with distance from the reservoir. But within 0.1–0.2 m, d-value decreased more strongly due to the effect of decreasing porosity at the gypsum dissolution front. With ongoing gypsum dissolution and ion transport into the reservoir, the pressure step and dissolution front moved to the right (Fig. 3 in supplementary material). This model prediction clearly demonstrated the two relevant clay properties determining d-value: total porosity (or, closely linked, dry density), and porewater chemistry.

After 114y (Fig. 8), the porewater chemistry across the core resembled the initial condition (except the tracer): free water concentrations were identical with the reservoir, but some Ca was still present in the Donnan porosity (on the exchanger, in the classic clay concept), which was barely visible (Ca increasing, Na decreasing from left to right; Ca: still 8 eq% of CEC at very right). Even after 1000 y of interaction with the Ca-free reservoir, Ca was present in the ppm range of CEC in the bentonite.

At this time, porewater and exchanger were virtually equal to initial condition (except the tracer), and the increased d-value (from initially

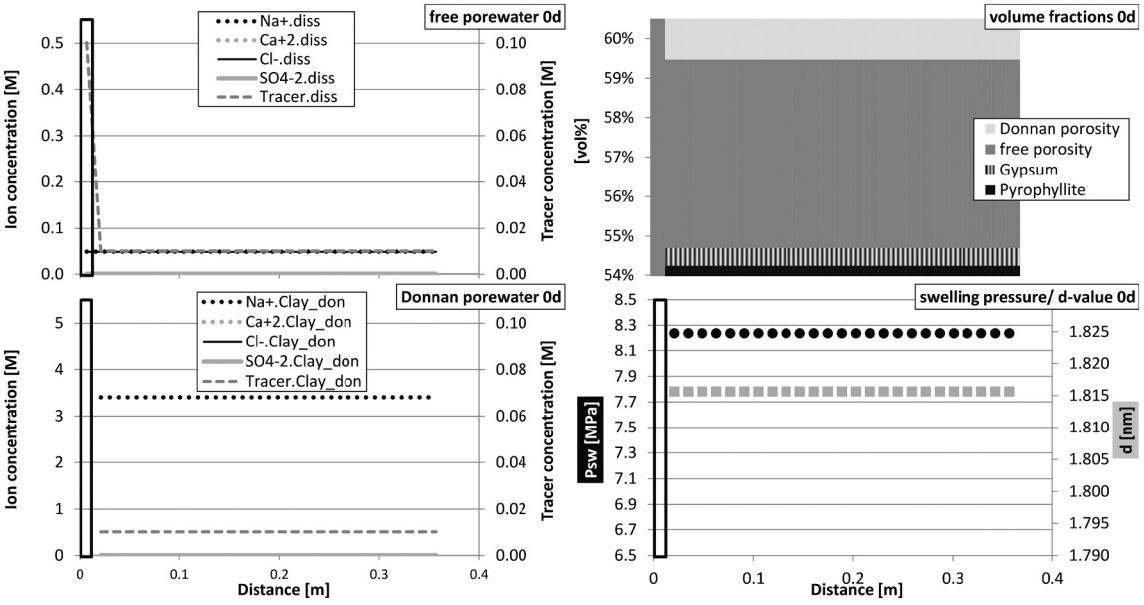

Fig. 6. Initial properties of a bentonite core in contact with a constant-concentration reservoir on the left (frame).

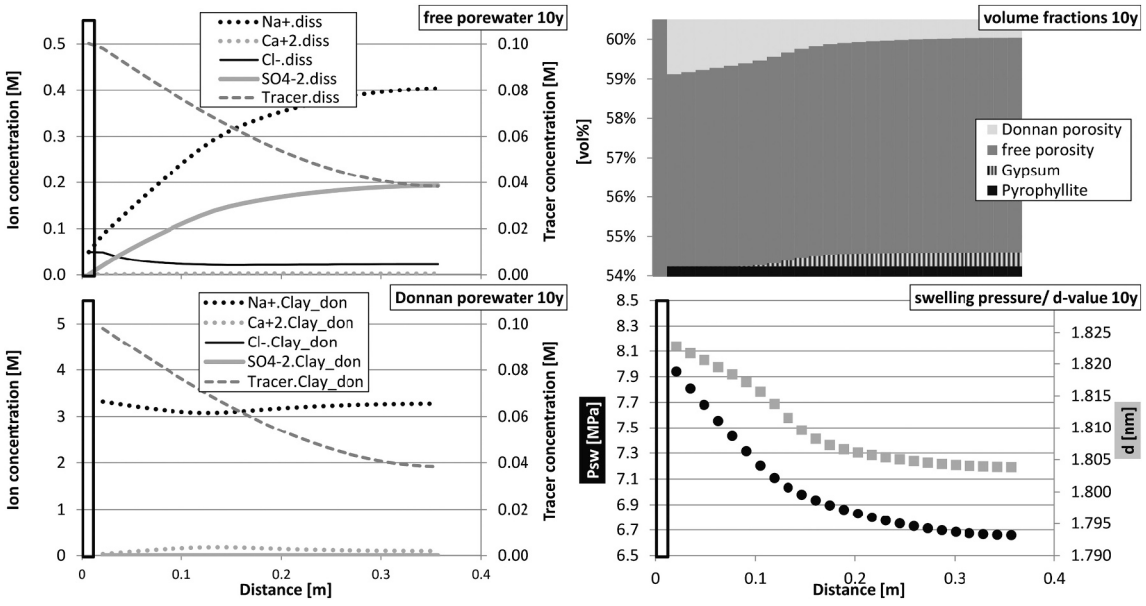

Fig. 7. Profiles across a bentonite core after 10 y of interaction with a constant concentration reservoir on the left (frame).

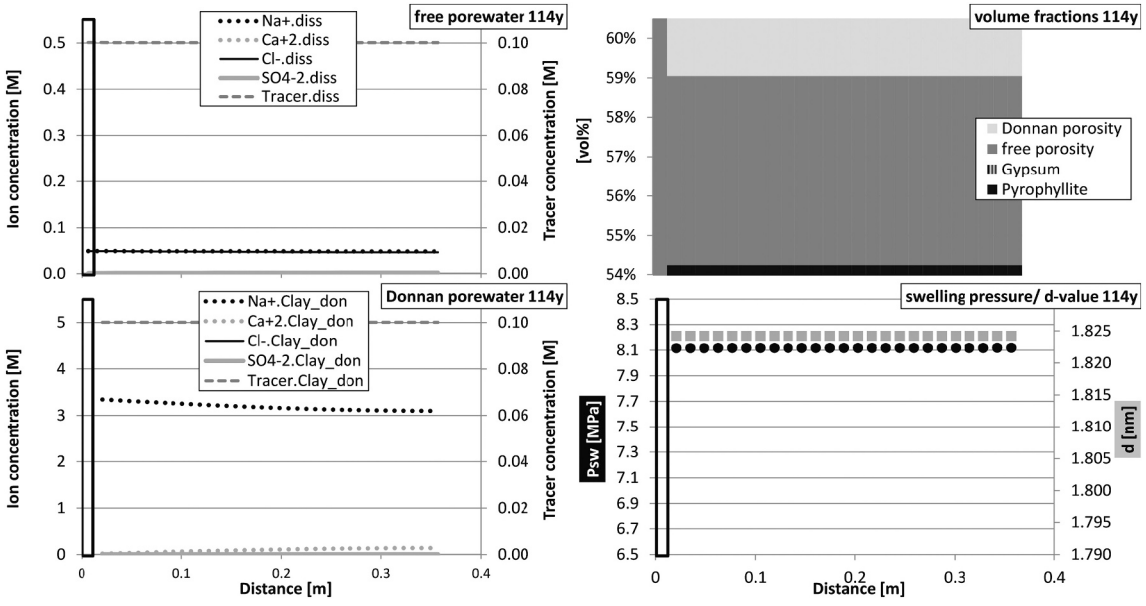

Fig. 8. Profiles across a bentonite core after 114 y of interaction with a constant concentration reservoir on the left (frame).

1.816 nm to 1.824 nm) and decreased swelling pressure (from 8.23 MPa to 8.12 MPa) could be attributed exclusively to the increased porosity caused by the dissolution of 0.46 vol% of gypsum (decreased EMDD from 1.408 g/cm^3 to 1.401 g/cm^3).

5. Discussion

The few parameters required for the chemomechanical coupling part of the code (Table 1) are well constrained by experimental measurements, except for elastic stiffness k. However, the sensitivity of the model results to the variation of k was found to be low. It was therefore decided to use in the simulations the values estimated in hydromechanical approaches by De la Morena et al. (2018), Navarro et al. (2015, 2017a, 2017b). The required reference measurement of montmorillonite swelling pressure and d-value at known dry density and zero ionic strength were taken from the same experimental datasets used for verification of physical code predictions (Holmboe et al., 2012; Karnland et al., 2006). The code can then predict the behaviour of saturated clays of various densities and equilibrated with different NaCl and $CaCl_2$ concentrations in good agreement with the limited experimental data. The swelling pressure measurements lack an error estimation. But the small cell volume containing the montmorillonite core of 4.8 cm^3 suggests a considerable influence of various boundary conditions. Similarly, the discrepancy in measured d-values between the different data sources implies rather large measurement uncertainties.

No MD or other data are available for the effect of sulphate or alternative anions on water retention or swelling pressure. The sulphate concentrations evolving in the model application presented in the section above were treated as the double concentration of Cl for the suction prediction in the CM coupling part of the code. Then the charge balance of a hypothetic MD system corresponding with the chemical conditions of the modelling example was maintained. Navarro et al. (2017a)

approximated osmotic suction proportional to the sum of activities of all ions present in the porosity domain, disregarding their charge. In turn, swelling pressures were often considered to depend on ionic strength, in addition to the cation occupancy. The disagreement in literature in choosing the actual parameter influencing the clay swelling behaviour (ionic strength, charge equivalent sum, concentration sum) indicates a knowledge gap in the clay swelling mechanism.

We are still far from a mechanistic description of swelling pressure and d-value. MD simulations indicated that, in terms of cation on the exchanger, ion radii and hydration energy are major parameters governing the swelling behaviour (Fayoyiwa et al., 2020a, 2020b), which were captured in this modelling approach for Na and Ca. Nevertheless, general trends of swelling pressure versus dry density (or d-value) were similar for all considered monovalent cations, and similar for the bivalent cations. This suggests, in a first approximation, to treat alternative monovalent cations as Na, and bivalent cations as Ca in the CM coupling part of the current model, if it is used for simulating systems beyond Na and Ca.

In the model application presented above, the porewater chemistries of initial condition and final equilibrium state were identical. The differences in swelling pressure and d-value could be exclusively attributed to the change in total porosity. In between, the swelling behaviour of the clay followed from overlying spatial and chemical mechanisms. A reactive transport simulation with a very simplified CM coupling approach predicted a slightly more complex scenario (Jenni and Mäder, 2018): the initial bentonite porewater (0.2 M ionic strength) was in equilibrium with gypsum, in contact with a dilute or brine water from the adjacent reservoir. Nevertheless, these older simulation results could be compared with the prediction here, because gypsum reaction rate and geometric factors G (see Eqs. (2) and (3)) were equal. Roughly 100 y of diffusive interaction between the constant concentration reservoir and the bentonite were needed to remove half of the gypsum, whereas in the current simulation, roughly 30 y are required. The faster gypsum removal at equal transport properties could be partially attributed to the larger chemical gradients between reservoir and bentonite porewater, which led to larger diffusive fluxes in case of the current simulation. In addition, the code used in the older approach (CrunchFlowMC beta version) suffered from an unsolved connectivity issue between the reservoir containing free porewater only and the two bentonite porosity domains. At such interfaces, the free porosity of the bentonite must connect to a fraction of the free porosity in the reservoir, and the Donnan porosity to the remaining free porosity in the reservoir. Tournassat and Steefel (2015) suggested approaches for the calculation of diffusive fluxes.

The simple geometry of the model applications enabled to run the codes on personal computers within reasonable calculation times. Because CrunchFlowMC automatically adapted the timestep length to meet the convergence criteria, calculation times strongly depended on the problem. Dilute porewaters involving small free porosity fractions led to small timesteps and calculation times in the range of hours per simulated year. In contrast, the ORCHESTRA simulation shown here run with a default timestep leading to calculation times around 30 seconds per simulated year. Timestep length can still be optimised, which will substantially decrease calculation times. However, only a study running equal problems can rigorously compare code performances.

6. Conclusions

The chemical environment of swelling clays affects their hydromechanical properties. The presented reactive transport model approach aimed at coupling the chemical composition of the porewater in the clay with its swelling pressure and volume fractions of the free and Donnan porosity domains.

For this purpose, data from molecular dynamics (MD) simulations was successfully upscaled and implemented into the chemomechanical coupling extension of ORCHESTRA. In this way, the experimentally derived water retention curve generally used in hydromechanical models was replaced with MD data.

The versatile new approach for modelling saturated swelling clays fully coupled porewater chemistry, exchanger population, diffusive transport, d-value (and closely linked, fractions of Donnan and free porosity), and swelling pressure. The presented simulation example demonstrated the coupling of all these properties or mechanisms. Although the example simulated a rather simple chemistry, the approach can be extended to more complex chemistries for which ORCHESTRA is commonly used, without significant increase in computational time to be expected. In addition to the general reactive transport parameters (porewater chemistry, mineralogy), the code can then predict changes in bentonite swelling pressure and transport behaviour caused by the interaction with the host rock, infiltrating groundwater, cement, or steel. For the performance prediction of alternative bentonites, specific MD data must be generated and physical reference properties measured.

Declaration of Competing Interest

The authors declare that they have no known competing financial interests or personal relationships that could have appeared to influence the work reported in this paper.

Acknowledgement

The study was financially supported by Posiva Oy.

Appendix A. Supplementary data

Supplementary data to this article can be found online at https://doi.org/10.1016/j.clay.2021.106274.

References

Akinwunmi, B., Hirvi, J.T., Kasa, S., Pakkanen, T.A., 2020a. Swelling pressure of Na- and Ca-montmorillonites in saline environments: a molecular dynamics study. Chem. Phys. 528, 110511.

Akinwunmi, B., Kporha, F.E.A., Hirvi, J.T., Kasa, S., Pakkanen, T.A., 2020b. Atomistic simulations of the swelling behaviour of Na-montmorillonite in mixed NaCl and $CaCl_2$ solutions. Chem. Phys. 533, 110712.

Alonso, E.E., Gens, A., Josa, A., 1990. A constitutive model for partially saturated soils. Geotechnique 40, 405–430.

Alt-Epping, P., Tournassat, C., Rasouli, P., Steefel, C.I., Mayer, K.U., Jenni, A., Mäder, U., Sengor, S.S., Fernández, R., 2015. Benchmark reactive transport simulations of a column experiment in compacted bentonite with multispecies diffusion and explicit treatment of electrostatic effects. Comput. Geosci. 1–16.

Berner, U., Kulik, D.A., Kosakowski, G., 2013. Geochemical impact of a low-pH cement liner on the near field of a repository for spent fuel and high-level radioactive waste. Phys. Chem. Earth 64, 46–56.

Chagneau, A., Tournassat, C., Steefel, C.I., Bourg, I.C., Gaboreau, S., Esteve, I., Kupcik, T., Claret, F., Schaefer, T., 2015. Complete restriction of $^{36}Cl^-$ diffusion by celestite precipitation in densely compacted illite. Environ Sci Technol Letters 2, 139–143.

De la Morena, G., Asensio, L., Navarro, V., 2018. Intra-aggregate water content and void ratio model for MX-80 bentonites. Eng. Geol. 246, 131–138.

Dixon, D.A., Chandler, N.A., Baumgartner, P., 2002. The influence of groundwater salinity and interfaces on the performance of potential backfilling materials. In: 6th International Workshop on Design and Construction of Final Repositories. ONDRAF/NIRAS, Brussels, Belgium.

Dueck, A., Goudarzi, R., Börgesson, L., 2018. Buffer homogenisation - status report 4. In: SKB Technical Report TR-17-04. www.skb.se. Stockholm, Sweden.

Fayoyiwa, A.D., Hirvi, J.T., Pakkanen, T.A., 2020a. Computational study of the roles of alkali cation species in the swelling pressure of smectites. Chem. Phys. Lett. 744, 137200.

Fayoyiwa, A.D., Hirvi, J.T., Pakkanen, T.A., 2020b. Roles of alkaline-earth cation species in the swelling pressure of smectites – a computational study. Chem. Phys. Lett. 753, 137602.

Fernández, R., Cuevas, J., Mäder, U.K., 2009. Modelling concrete interaction with a bentonite barrier. Eur. J. Mineral. 21, 177–191.

Flury, M., Gimmi, T., 2002. Solute diffusion. In: Dane, J.H., Topp, G.C. (Eds.), Methods of Soil Analysis, Part 4: Physical Methods. Soil Science Society of America, Inc., Madison, Wisconsin, USA.

Glaus, M.A., Frick, S., Rosse, R., Van Loon, L.R., 2010. Comparative study of tracer diffusion of HTO, Na-22$^{(+)}$ and Cl-36$^{(-)}$ in compacted kaolinite, illite and montmorillonite. Geochim. Cosmochim. Acta 74, 1999–2010.
Hoffmann, C., Alonso, E.E., Romero, E., 2007. Hydro-mechanical behaviour of bentonite pellet mixtures. Phys. Chem. Earth 32, 832–849.
Holmboe, M., Wold, S., Jonsson, M., 2012. Porosity investigation of compacted bentonite using XRD profile modeling. J. Contam. Hydrol. 128, 19–32.
Jenni, A., Mäder, U., 2018. Coupling of chemical and hydromechanical properties in bentonite. Appl. Geochem. 97, 147–156.
Jenni, A., Gimmi, T., Alt-Epping, P., Mäder, U., Cloet, V., 2017. Interaction of ordinary Portland cement and Opalinus Clay: dual porosity modelling compared to experimental data. Phys. Chem. Earth Parts A/B/C 99, 22–37.
Jenni, A., Wersin, P., Thoenen, T., Baeyens, B., Ferrari, A., Gimmi, T., Mäder, U., Marschall, P., Hummel, W., Leupin, O., 2019. Bentonite backfill performance in a high-level waste repository: A geochemical perspective. In: Nagra Technical Report NTB 19–03. Switzerland, Wettingen.
Karnland, O., Olsson, S., Nielsson, U., 2006. Mineralogy and sealing properties of various bentonites and smectite-rich clay materials. In: SKB Technical Report TR-06-30. www.skb.se. Stockholm, Sweden.
Karnland, O., Nilsson, U., Weber, H., Wersin, P., 2008. Sealing ability of Wyoming bentonite pellets foreseen as buffer material - laboratory results. Phys. Chem. Earth, Parts A/B/C 33 Supplement 1, S472–S475.
Kosakowski, G., Berner, U., 2013. The evolution of clay rock/cement interfaces in a cementitious repository for low- and intermediate level radioactive waste. Phys. Chem. Earth 64, 65–86.
Kozaki, T., Saito, N., Fujishima, A., Sato, S., Ohashi, H., 1998. Activation energy for diffusion of chloride ions in compacted sodium montmorillonite. J. Contam. Hydrol. 35, 67–75.
Kozaki, T., Fujishima, A., Sato, S., Ohashi, H., 1998b. Self-diffusion of sodium ions in compacted sodium montmorillonite. Nucl. Technol. 121, 63–69.
Kozaki, T., Liu, J., Sato, S., 2008. Diffusion mechanism of sodium ions in compacted montmorillonite under different NaCl concentration. Phys. Chem. Earth 33, 957–961.
Kozaki, T., Sawaguchi, T., Fujishima, A., Sato, S., 2010. Effect of exchangeable cations on apparent diffusion of Ca(2+) ions in Na- and Ca-montmorillonite mixtures. Phys. Chem. Earth 35, 254–258.
Lasaga, A.C., 1981. Transition state theory. Rev. Mineral. Geochem. 8, 135–168.
Lasaga, A.C., 1984. Chemical kinetics of water-rock interactions. J. Geophys. Res. 89, 4009–4025.
Marty, N.M., Bildstein, O., Blanc, P., Claret, F., Cochepin, B., Gaucher, E., Jacques, D., Lartigue, J.-E., Liu, S., Mayer, K.U., Meeussen, J.L., Munier, I., Pointeau, I., Su, D., Steefel, C., 2015. Benchmarks for multicomponent reactive transport across a cement/clay interface. Comput. Geosci. 1–19.
Meeussen, J.C.L., 2003. Orchestra: an object-oriented framework for implementing chemical equilibrium models. Environ. Sci. Technol. 37, 1175–1182.
Meeussen, J.C.L., 2021. Orchestra. Geochem. Model. http://orchestra.meeussen.nl/.
Navarro, V., Asensio, L., De la Morena, G., Pintado, X., Yustres, A., 2015. Differentiated intra- and inter-aggregate water content models of MX-80 bentonite. Appl. Clay Sci. 118, 325–336.
Navarro, V., De la Morena, G., Yustres, A., Gonzalez-Arteaga, J., Asensio, L., 2017a. Predicting the swelling pressure of MX-80 bentonite. Appl. Clay Sci. 149, 51–58.
Navarro, V., Yustres, A., Asensio, L., De la Morena, G., Gonzalez-Arteaga, J., Laurila, T., Pintado, X., 2017b. Modelling of compacted bentonite swelling that accounts for salinity effects. Eng. Geol. 223, 48–58.
Navarro, V., Yustres, Á., Jenni, A., De la Morena, G., Asensio, L., López-Vizcaíno, R., Cabrera, V., Wersin, P., Mäder, U., Muuri, E., Niskanen, M., Akinwunmi, B., Hirvi, J. T., Pakkanen, T.A., 2021. Molecular dynamics data for modelling the microstructural behaviour of compacted sodium bentonites. Appl. Clay Sci. 201, 105932.
Palandri, J.L., Kharaka, Y.K., 2004. A compilation of rate parameters of water-mineral interaction kinetics for application to geochemical modeling. In: U.S.G (Ed.), Survey. U.S. Geological Survey, Washington, USA.
Samper, J., Mon, A., Montenegro, L., 2018. A revisited thermal, hydrodynamic, chemical and mechanical model of compacted bentonite for the entire duration of the FEBEX in situ test. Appl. Clay Sci. 160, 58–70.
Seiphoori, A., Ferrari, A., Laloui, L., 2014. Water retention behaviour and microstructural evolution of MX-80 bentonite during wetting and drying cycles. Geotechnique 64, 721–734.
Steefel, C.I., Appelo, C.A.J., Arora, B., Jacques, D., Kalbacher, T., Kolditz, O., Lagneau, V., Lichtner, P.C., Mayer, K.U., Meeussen, J.C.L., Molins, S., Moulton, D., Shao, H., Šimůnek, J., Spycher, N., Yabusaki, S.B., Yeh, G.T., 2014. Reactive transport codes for subsurface environmental simulation. Comput. Geosci. 1–34.
Sun, L.L., Hirvi, J.T., Schatz, T., Kasa, S., Pakkanen, T.A., 2015. Estimation of montmorillonite swelling pressure: a molecular dynamics approach. J. Phys. Chem. C 119, 19863–19868.
Tournassat, C., Appelo, C.A.J., 2011. Modelling approaches for anion-exclusion in compacted Na-bentonite. Geochim. Cosmochim. Acta 75, 3698–3710.
Tournassat, C., Steefel, C.I., 2015. Ionic transport in nano-porous clays with consideration of electrostatic effects. Rev. Mineral. Geochem. 80, 287–329.
Van Loon, L.R., Glaus, M.A., Müller, W., 2007. Anion exclusion effects in compacted bentonites: Towards a better understanding of anion diffusion. Appl. Geochem. 22, 2536–2552.
Villar, M.V., Gomez-Espina, R., Gutiérrez-Nebot, L., 2012. Basal spacings of smectite in compacted bentonite. Appl. Clay Sci. 65-66, 95–105.
Wallis, I., Idiart, A., Dohrmann, R., Post, V., 2016. Reactive transport modelling of groundwater-bentonite interaction: effects on exchangeable cations in an alternative buffer material insitu test. Appl. Geochem. 73, 59–69.
Wersin, P., Kumpulainen, S., 2017. Definition of Reference Backfill Characteristics for TURVA-2020. Technical Memorandum, Posiva.
Yustres, A., Jenni, A., Asensio, L., Pintado, X., Koskinen, K., Navarro, V., Wersin, P., 2017. Comparison of the hydrogeochemical and mechanical behaviours of compacted bentonite using different conceptual approaches. Appl. Clay Sci. 141, 280–291.
Zheng, L., Xu, H., Rutqvist, J., Reagan, M., Birkholzer, J., Villar, M.V., Fernández, A.M., 2020. The hydration of bentonite buffer material revealed by modeling analysis of a long-term in situ test. Appl. Clay Sci. 185, 105360.